

Soma Vesztergom\*, Noémi Kovács, Mária Ujvári, and Gyözö G. Láng

# Apparatus and methods for using a rotating ring–disk electrode with potentiodynamic control of both working electrodes

Aufbau und Anwendungen einer rotierenden Ringscheibenelektrode mit potentiodynamischer Kontrolle beider Arbeitselektroden

<https://doi.org/10.1515/teme-2016-0083>

Received December 19, 2017; revised May 17, 2017; accepted May 18, 2017

**Abstract:** When studying electrochemical processes, one of the most widely used methods of determining the reaction pathway is an electrochemical assay of products using a rotating ring–disk electrode (RRDE). An RRDE tip consists of two electron conducting parts: a centrally located disk and a ring around it. When brought into contact with an electrolyte solution, the disk and the ring both form electrodes, the potentials of which can be independently controlled by a bi-potentiostat. When the tip is rotated, reactants from the solution arrive at the disk where they undergo an electrode reaction (oxidation or reduction) at a given rate, depending on the rotation speed. The formed products leave the disk surface and due to forced convection make their way towards the ring electrode where they can undergo another electrode reaction and can thus be detected. Normally, one applies potentiostatic control to at least one of the electrodes when carrying out an RRDE experiment; albeit the simultaneous potentiodynamic perturbation of the electrodes offers an increased applicability range. This paper presents the construction of a measuring system capable for the “bi-potentiodynamic” perturbation of two working electrodes, and demonstrates the use of such methods in case of a few chosen example systems.

**Keywords:** Electrochemistry, dual cyclic voltammetry, 3D map of reaction products, single-frequency capacitance, PEDOT.

**Zusammenfassung:** Die rotierende Ringscheibenelektrode (rotating ring-disk electrode, RRDE) ist eine der meist genutzten analytischen Methoden zur Ermittlung von Reaktionswegen und Zwischenprodukten elektrochemischer Umsetzungen. Der planare Aufbau besteht aus einer zentral angeordneten Scheibenelektrode und einer sie umgebenden Ringelektrode. Eingetaucht in eine Elektrolytlösung können mit geeigneten Potentiostaten beide Elektroden separat kontrolliert und angesteuert werden. Wird der Elektrodenaufbau in Rotation gebracht, werden die Reaktanden in Richtung auf die Elektrode bewegt und dort einer elektrochemischen Reaktion (Oxidation oder Reduktion) unterworfen. Der Umsatzrate ist von der Rotationsgeschwindigkeit abhängig. Die gebildeten Produkte werden durch die erzwungene Konvektion an die Ringelektrode transportiert und können dort einer weiteren elektrochemischen Umsetzung unterzogen und analysiert werden. In der Regel wird eine der beiden Elektroden bei einem RRDE-Experiment potentiostatisch betrieben, obwohl eine simultane potentiodynamische Nutzung beider Elektroden eine Erweiterung des elektroanalytischen Anwendungsspektrums erlaubt. Diese Veröffentlichung stellt die Konstruktion eines Messsystems vor, welches für die simultane „bi-potentiometrische“ dynamische Anregung beider Elektroden genutzt werden kann und weist die Eignung dieses Aufbaus an einigen exemplarischen Untersuchungen nach.

**Schlüsselwörter:** Elektrochemie, simultane Voltammetrie, 3D-Karte von Reaktionsprodukten, Einzelfrequenzkapazität, PEDOT.

**\*Corresponding author: Soma Vesztergom**, Eötvös Loránd University, Department of Physical Chemistry, Pázmány Péter sétány 1/A, 1117 Budapest, Hungary, e-mail: [vesztergom@chem.elte.hu](mailto:vesztergom@chem.elte.hu), <http://orcid.org/0000-0001-7052-4553>

**Noémi Kovács, Mária Ujvári, Gyözö G. Láng:** Eötvös Loránd University, Department of Physical Chemistry, Pázmány Péter sétány 1/A, 1117 Budapest, Hungary

## 1 Introduction

In chemical industry, civil engineering, environmental protection and corrosion testing electrochemical methods [1, 2] are very often used techniques of chemical characterization. This is due to the relatively low cost of the measuring equipment and the availability of standardized techniques. One of the most often used instruments in both electrochemical research and in applied electrochemistry is the potentiostat.

A potentiostat is a device used for keeping the potential of a working electrode (the electrode under study) at a constant level with respect to a reference electrode by adjusting the current at an auxiliary electrode. It consists of an electric circuit which provides voltage control by the use of operational amplifiers (Figure 1). Depending on their design, potentiostats may be used not only to stabilize a constant potential but also to control the potential of the working electrode according to a time-dependent voltage waveform. Bi- or multi-potentiostats are similar circuits that can control the potential of two or more working electrodes (with respect to the same reference and by using one auxiliary electrode).

Nowadays potentiostats and galvanostats designed for an everyday laboratory use are commercially available products. These instruments provide a straightforward way of making standard electrochemical and electroanalytical measurements, even for an untrained staff. As a result of the fact that the instruments are highly automated—controlling the device, as well as visualizing and evaluating the measured data can usually be carried out by using software—the job of the operator is simplified to a great extent.

The advances in electrochemical instrumentation have very significantly improved the reproducibility, accuracy and speed with which electrochemical experiments can be performed. However, in the pursuit of fulfilling the needs of applied science, the manufacturers of potentiostats often neglect the demands of fundamental research [3]. The primary instruments of electrochemical research more and more become “black boxes” and only limited efforts are devoted to the design of new instruments. Consequently, methodological developments often require the design of new, “home-made” measuring systems.

In this paper the construction and application of a new electrochemical measuring system [4], developed in our research group, is described. By the use of the presented measuring system, significant improvements [4–8] have been made to electrochemical methods based on the use of rotating ring–disk electrodes (RRDEs). A common

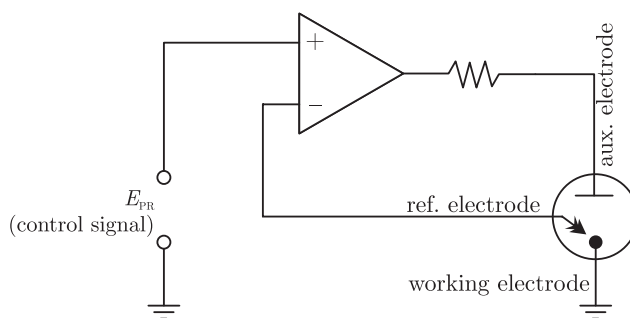


**Figure 1:** A simplified potentiostat circuit. The operational amplifier realizes a current flow between the auxiliary and the working electrodes so that the potential difference between the reference and the working electrodes would match the voltage of the control signal.

feature of these methods is that they apply potentiodynamic control to *both* working electrodes at the same time.

The advantages of dual potentiodynamic control were first made use of for the investigation of gold dissolution upon potential excursions to the region of oxide formation, for which two techniques—phase-shifted dual cyclic voltammetry [5] and synchronous dual cyclic voltammetry [7]—have been utilized. The latter technique, as is going to be shown, yields results that are more easily quantifiable; however both techniques are superior to “standard” RRDE techniques in terms of reproducibility. While in standard RRDE measurements the surface of the collector electrode loses sensitivity due to long-time conditioning at a certain potential, in case of dual voltammetry the ring potential is continuously scanned, thus the ring surface is under constant “electrochemical polishing”.

Dual potentiodynamic control is also expedient in the detection of reaction products at a large potential range, as it was shown for the case of oxygen reduction occurring on gold [6, 7]. This reaction yields products (primarily  $\text{H}_2\text{O}_2$ ) that can undergo faradaic reaction at the collector (ring) electrode surface.

The original workstation (described in Reference [4]) has recently undergone serious improvements and—by the implementation of on-the-fly Fourier analysis—can now be used in an essentially non-faradaic detection mode as well, when one carries out single-frequency capacitance measurements on the ring [8].

The aim of this paper is to review results that became available by the application of dual potentiodynamic control to the two working electrodes of an RRDE. For readers who are not familiar with RRDE methods, a short introduction is given in the next section. For a more basic introduction to electrochemistry and electrochemical

measurements in general, the reader is directed to other sources [1, 2].

### 1.1 Electrochemical experiments with rotating ring–disk electrodes

When studying the mechanisms of electrochemical processes, one of the most convenient and widely used methods of determining the reaction pathway is an electrochemical assay of the reaction products using a rotating ring–disk electrode (RRDE) [9, 10]. The first RRDE was developed by Frumkin, Levich and their coworkers in 1959 [11].

As a typical example of so-called generator–collector assemblies, an RRDE tip consists of two electron conducting parts: a generator, the centrally located disk, and the collector, the ring around it. Disk and ring are separated by a gap that is filled with the same insulating material that is used for constructing the outer shroud (Figure 2). The tip is immersed into a solution of interest already containing the reference and the auxiliary electrode and all four electrodes are connected to a bi-potentiostat [12] through separate leads.

The cylindrical symmetry of the RRDE allows for an accurate control over the mass transfer rate of electroactive species dissolved in the solution. When the tip is rotated, reactants from the solution arrive at the disk where they undergo an electrode reaction (oxidation or reduction) at a given rate, depending on the speed of rotation. Products formed at the disk electrode leave the disk surface and due to forced convection make their way towards the ring electrode. The potential of the ring,  $E_{\text{ring}}$ , can be regulated independently from the potential of the disk,  $E_{\text{disk}}$ ; that is, when an appropriate value of  $E_{\text{ring}}$  is used, the portion of disk reaction products reaching the ring electrode can undergo there another electrode reaction and can thus be detected.

RRDEs have many advantages but a few drawbacks as well. For example, the collection efficiency of other generator–collector devices (such as microelectrode arrays) is higher, which gives such systems an advantage in detecting small amounts of generator electrode products. Nevertheless, it is a considerable advantage of RRDEs that in experiments employing this technique hydrodynamic constraints assure that the current-potential characteristics of the generator electrode remain unaffected by the presence of the collector. This is not the case when using other devices, microelectrode systems included.

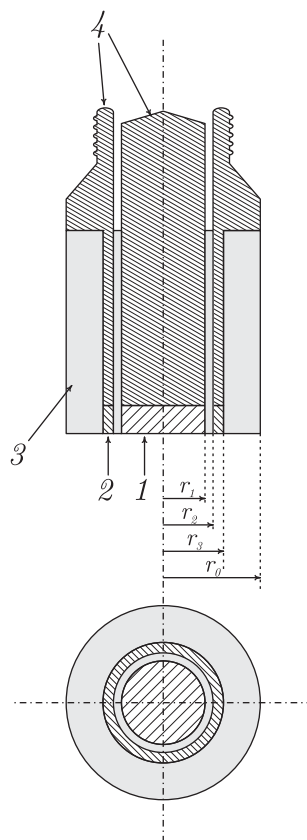


**Figure 2:** Sketch of a rotating ring–disk electrode. 1: disk electrode material, 2: ring electrode material, 3: insulator, 4: metal support,  $r_1$ : disk radius,  $r_2$ : inner ring radius,  $r_3$ : outer ring radius,  $r_0$ : overall radius of the tip.

So far, when RRDEs were employed to detect intermediates of electrode reactions, mainly one of the following techniques were used:

- A current-potential curve was recorded at the disk while the ring potential was held at a constant value where the intermediates or products are reduced or oxidized.
- The disk was held at a potential where intermediates or electroactive products were formed and the ring was maintained at a potential at which they have undergone electron transfer.
- The disk was held at a potential where the reaction of interest took place, and a current-potential curve was then recorded at the ring.
- The subject of observation was the transient shielding of the ring current for the electrolysis of a species upon stepping the disk potential to a value where this species was adsorbed.

The common feature of all the above techniques was that the potential of at least one of the two electrodes was held constant during the experiment. However, independent and dynamic potential programs can also be applied (simultaneously) to the disk and the ring electrodes and when appropriate potential programs are applied, the se-

lectivity and sensitivity of RRDE systems can significantly be increased [5].

Unfortunately, almost all the commercial software available today support only the traditional techniques listed above; thus, carrying out dual potentiodynamic measurements is, from an instrumentation point of view, not straightforward. The electrochemical workstation presented in this paper provides solutions for the dynamic and simultaneous control of two working electrodes, thereby making it possible to carry out unique electrochemical measurements.

## 2 Design of the measuring system

The operating principle of the measuring system (Figure 3) is based on the use of a bi-potentiostat to regulate the potentials of the disk and ring electrodes of an RRDE simultaneously, according to analogue controlling waveforms. These are provided by high speed, high resolution digital-to-analogue converters. In the meantime, the disk and ring potentials as well as the disk and ring currents are monitored at a high sampling rate by the use of analogue-to-digital converters. The workstation consists of the following hardware modules:

- A 4-electrode electrochemical cell, holding an RRDE as well as an auxiliary and a reference electrode. The RRDE can be rotated at a given rate by utilizing a PINE AFMSRCE electrode rotator unit.
- A bi-potentiostat is used to control the potentials of the disk and ring electrodes independently and to measure the electrode potentials and currents.
- Two software-controlled National Instruments PCI data acquisition cards installed in a computer are used to generate analogue controlling waveforms going into the bi-potentiostat, and to measure the output signals coming out of it.

### 2.1 Primary devices: bi-potentiostats

Modern bipotentiostats substantially differ from that presented in 1967 by Napp et al. [12]. In the past few decades, several improvements have been made to these devices, which resulted in a higher bandwidth, stability of response and convenience. A simplified circuit of a modern bi-potentiostat (PINE AFRDE5, [13]) is shown in Figure 4.

The circuitry of the potentiostatic control of the disk electrode consists of the potential follower PF1 and the control amplifier CA1 (the input of which is connected to the auxiliary electrode), and the current-to-voltage

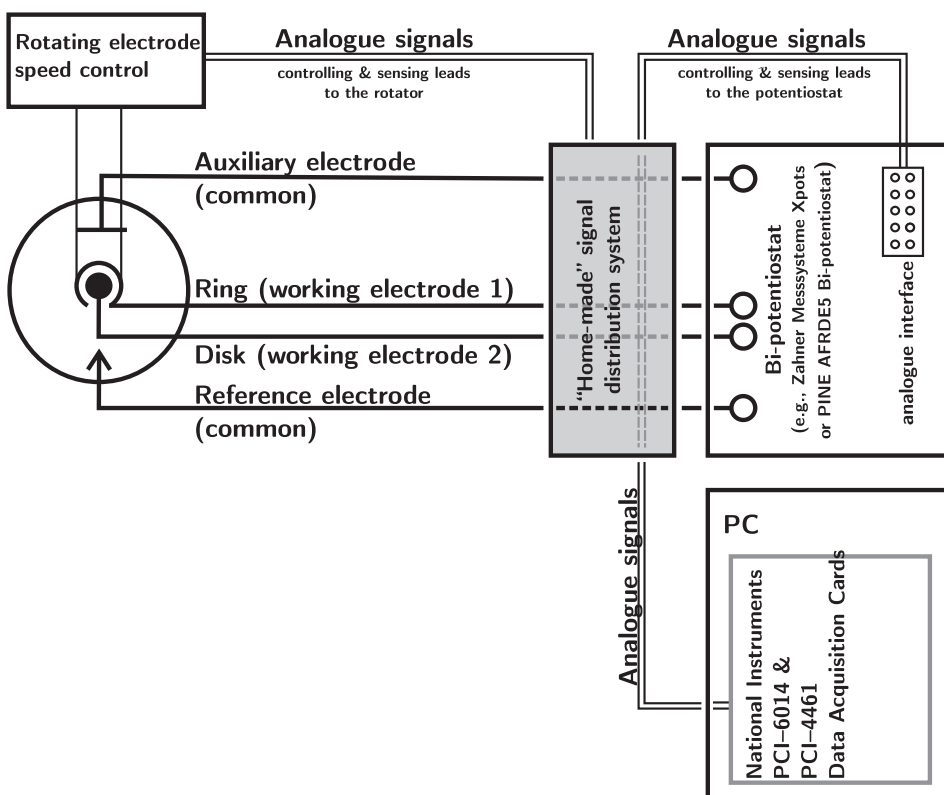
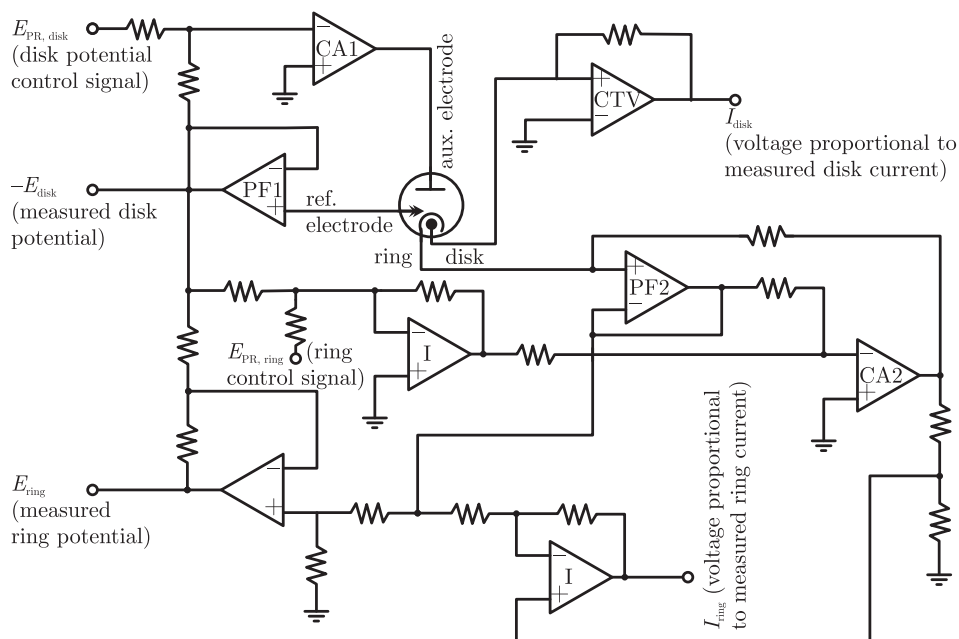


Figure 3: Scheme of the measuring system.



**Figure 4:** Circuit schematics of a bi-potentiostat coupled to an electrochemical cell holding an RRDE, an auxiliary and a reference electrode.

converter CTV. Serving as a current sink, CTV keeps the disk electrode at virtual ground by means of its current feedback loop; meanwhile, the amplifier CA1 maintains the difference between the disk and the reference electrode at the desired value. The circuitry required for the potentiostatic control of the second electrode (the ring) consists of the potential follower PF1, the inverter I, the control amplifier CA2 and the potential follower PF2. The role of CA2 is to make the potential difference between the ring electrode and the reference electrode equal to the voltage of the excitation signal.

As it can be seen in Figure 4, the auxiliary electrode is included in the control loops of both working electrodes, the current that flows through it is thus the algebraic sum of the disk and ring currents. By the application of a circuit like this, simultaneous potential control of the two working electrodes can be achieved. In many cases however, an equally efficient bipotentiostatic control can also be achieved by using two “single” potentiostats instead of a bipotentiostat.

The technical feasibility of this approach depends on the grounding concepts of the devices; that is, two or more potentiostats can be used in a multi-potentiostat assembly provided that their circuits ground the auxiliary (or, alternatively, the reference) and not the working electrode. For example, the XPot potentiostats manufactured by Zahner Messsysteme, Kronach, Germany [14] can be operated by placing the auxiliary electrode to ground, thus these devices can be used to create a bipotentiostatic setup.

## 2.2 Automated control and measurement

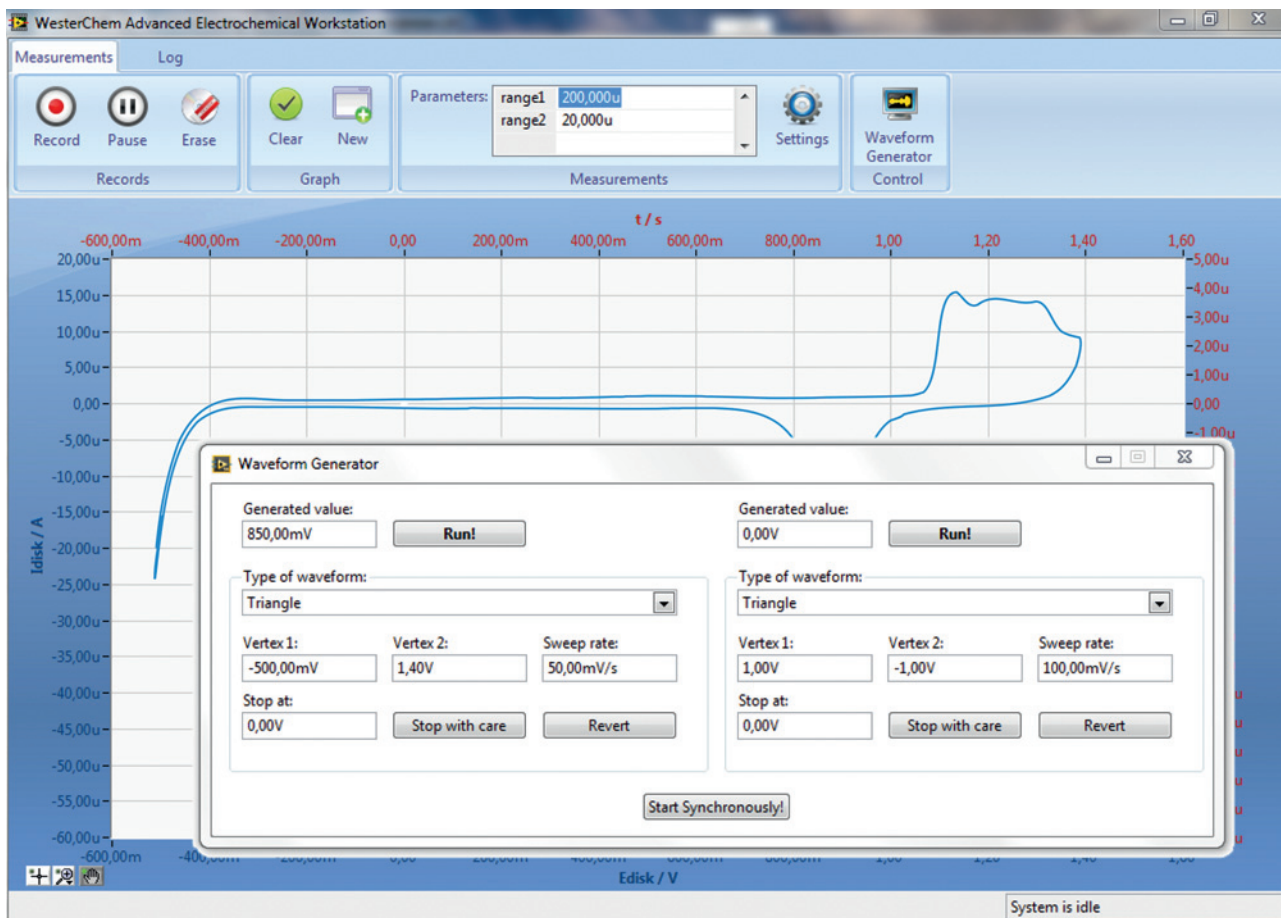
Our measuring system extensively relies on the various functionalities provided by the PCI-4461 [15] and PCI-6014 [16] data acquisition (DAQ) devices from National Instruments. These are used for generating and measuring analogue voltage signals: PCI-4461 is a high accuracy DAQ module with 24 bits resolution, 204.8 kS/s maximal sampling rate, 2 analogue input and 2 analogue output channels, while PCI-6014 is a DAQ module with 16 bits resolution, 200.0 kS/s maximal sampling rate, 2 analogue output and 8 differential analogue input channels. The main tasks of the DAQ devices are described in Table 1. The software controlling the experiments was written in the LabVIEW programming language [17].

When using the measuring system, the software continuously monitors the measured data and stores them in the memory or on a hard drive. The measurements can be visualized in real-time by using graphs of different kind. Multiple graph windows can be viewed together at the same time, with each graph customized according to the needs of the user: different quantities can be assigned to the axes, the range of which are adjustable (or auto-scaled). Moreover, there are various options for zooming and panning the graphs as well.

The graphical interface (Figure 5) has a user-friendly design: adjusting the experimental parameters, as well as changing the system settings are made straightforward by using a so-called “Ribbon” structure, context menus and keyboard short-cuts. Saving the measured results is possible in an ASCII-coded format but the software also

**Table 1:** Tasks of the different IO channels.

Device and channel	Task	Timing
PCI-4461 AO0 and AO1	Analogue output channels responsible for the synchronous generation of voltage waveforms. The waveforms are used to control the potentials of the disk and the ring electrodes, respectively. Usual sampling rate: 100 kS/s, resolution: 24 bits at 10 V.	continuous (time-critical)
PCI-6014 AI0..AI13	Analogue input channels used for monitoring the disk potential, disk current, ring potential, ring current, and rotation rate values, respectively. Usual sampling rate: 80 kS/s, resolution: 16 bits at 10 V. During post-processing, the measured data are made subject to an averaging which results in a smaller (typically 25 S/s) data acquisition rate. Due to the large factor of averaging, the measurements are of extremely low noise.	continuous (time critical)
PCI-6014 DIO0..DIO31	Digital lines with values of 5 V (true) or 0 V (false). These lines are connected to a home-made circuit and are responsible for various tasks, such as switching the entire cell or a given electrode on or off from the potentiostat, etc. If the applied potentiostat allows, these lines can also be used to maintain digital communication with the device firmware.	on-demand (bound to a user-action event in software)
PCI-6014 AO0	Analogue output channel that can be set to a given voltage value from the software to control the rotation rate of the RRDE. Resolution: 16 bits at 10 V, a value of 10 V results in a rotation rate of 10 000 min <sup>-1</sup> of the PINE model AFMSRCE rotator.	on-demand (bound to a user-action event in software)

**Figure 5:** Screenshot of the software controlling the measuring system. The main window containing a graph with measurement results is shown in the background. The window used for waveform generation is the one in the foreground.

provides an option for saving the “raw” (unaveraged) data in the form of binary-coded files. The saved data can later be analysed and evaluated; however, since the measuring system was designed for non-standard measurements, the evaluation of the data often requires special algorithms [6]. These algorithms are implemented in additional program modules.

### 3 RRDE experiments based on “dual potentiodynamic perturbation” techniques

The fact that the potentials of the disk and ring electrodes can be controlled independently and synchronously according to time-varying waveforms makes our measuring system capable of carrying out non-standard RRDE experiments [4–8] in which both the disk and the ring electrodes are under potentiodynamic (rather than potentiostatic) control. In what follows we give a few illustrative examples in order to demonstrate the advantages of dual “potentiodynamic perturbation” as applied to rotating ring-disk electrodes.

#### 3.1 Investigations on the reduction of the surface oxide of gold

**Experimental.** For the experiments described in this section “PINE AFE7R8” RRDE tips (collection efficiency: 22%) were used; both the disk (geometric surface area:  $0.1642\text{ cm}^2$ ) and the ring (geometric surface area:  $0.0370\text{ cm}^2$ ) were made of polycrystalline gold. The gap size between the ring and the disk was  $178\text{ }\mu\text{m}$ . The electrode surface was firmly polished with diamond suspensions (Struers) down to a diamond particle size of  $0.1\text{ }\mu\text{m}$ . The RRDE tip was then rinsed with pure ethanol, and in order to thoroughly remove all traces of contamination from the surface, it was cleaned ultrasonically for several minutes and washed extensively with ultrapure water. Every glass parts used in the experiments were immersed in Caro’s acid, rinsed in de-ionized water, and cleaned by steam. The measurements were carried out by bringing the RRDE in contact with  $0.5\text{ mol dm}^{-3}$  sulphuric acid solution. The electrochemical cell contained a separate reference compartment being connected to the cell by a Luggin capillary positioned  $\sim 1\text{ mm}$  below the RRDE surface. A gold plate with large surface was used as an auxiliary electrode, and a saturated calomel electrode (SCE) was applied as a reference. The sulphuric

acid solutions were made by dilution of concentrated sulphuric acid (Merck) with Milli-Q water. In order to remove any traces of dissolved oxygen, the solution was vigorously purged with a pure argon flow before actual measurements and an Ar blanket was maintained during the measurements.

It is well known from literature [18, 19] that during the reduction of the surface oxide layers of a gold electrode, oxidized gold species can leave the electrode surface. These species can be detected on the ring electrode of an RRDE at ring potentials lower than that of the oxide reduction peak seen on gold cyclic voltammograms (CVs) [18].

The traditional technique of detecting the reducible species using a gold disk/gold ring RRDE is to record cyclic voltammetric curves at the disk (Figure 6(a)), while keeping the ring electrode at an appropriately chosen, constant potential ( $0\text{ V vs. SCE}$ , Figure 6(b)).

As shown in Figure 6, two small cathodic peaks can be observed in the measured ring current curves. These peaks (denoted with P1 and P2 in Figures 6(b) and (c)) appear in parallel with the reduction of the surface oxide layer and the formation of the surface oxide, respectively. However, as it is clearly visible in Figure 6, the intensity of the detected peaks significantly decreases with the number of potential cycles applied to the disk. As in the meantime the disk CVs themselves do not change, this indicates that the electrocatalytic activity of the ring electrode decreases remarkably with time (most probably due to contaminations from the solution).

This issue, which makes the reproducibility (and also the quantitative interpretation) of the measurements questionable, can be successfully overcome by the simultaneous application of dual dynamic perturbing waveforms to both the disk and ring electrodes, as illustrated by Figure 7.

The measurements presented in Figure 7 were carried out by recording cyclic voltammograms not only at the disk, but also at the ring electrode at the same time. Similarly to the measurements presented before, the disk was polarized at a rate of  $50\text{ mV/s}$  between vertices of  $-500$  and  $1400\text{ mV vs. SCE}$ . Simultaneously, the ring CVs were taken within the boundaries of the double-layer region, between  $200$  and  $675\text{ mV}$ , at a rate of  $12.5\text{ mV/s}$ . The triangular waveforms controlling the potentials of the disk and ring electrodes were therefore synchronous (meaning that they both had a frequency of  $f = \frac{1}{76}\text{ Hz}$ ), and a phase shift of  $180^\circ$  was introduced in-between them (see the inset of Figure 7).

It can be seen in Figure 7 that both the disk and the ring CVs have a different shape when the electrode is

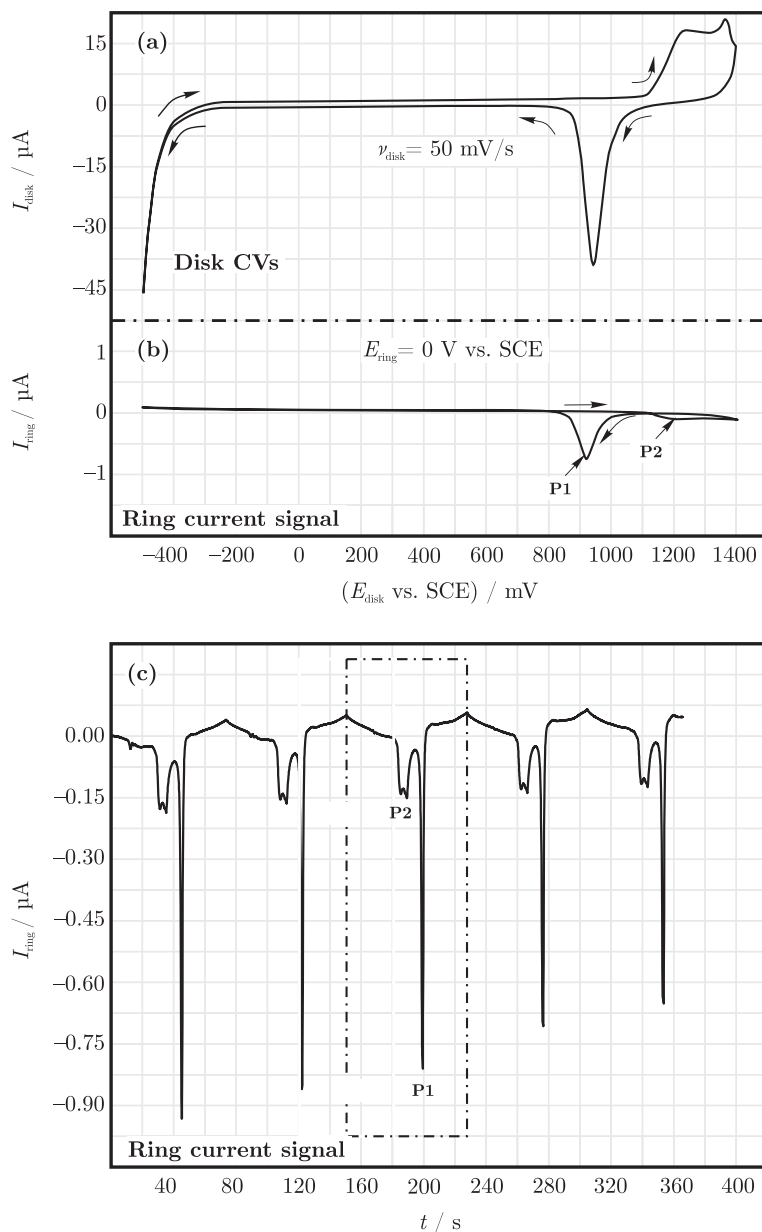


**Figure 6:** (a) Cyclic voltammograms measured on the disk electrode between vertices of 1400 and  $-500$  mV at a sweep-rate of  $50$  mV/s. (c) The ring current is recorded in parallel with measuring the CVs of the disk. A segment of the measured ring current is shown as a function of the disk potential in (b). Rotation rate:  $500$  min $^{-1}$ , ring potential:  $0$  V vs. SCE.

stagnant (non-rotating, marked with a green dashed line) and when it is rotated at a frequency of  $500$  min $^{-1}$  (solid red line). It can also be seen in Figure 7 that if the RRDE tip is rotated (red curve), the two peaks we have seen before in Figure 6 (marked with P1 and P2) can be observed in the ring CV. Since the triangular perturbations of the two electrodes are synchronous (they are of the same frequency) and they are shifted with  $180^\circ$  with respect to each other, the points of each curves in Figure 7 with a matching horizontal coordinate coincide with each other in time. By subtracting the ring currents measured at a stagnant electrode from those measured when the electrode is rotating (i.e., by calculating the difference of the red and the

green curves in Figure 7(b)), the plot in Figure 7(c) can be created.

In this representation the intensities of the peaks P1 and P2 are much higher compared to the conventional RRDE results presented in Figure 6, and the resolution is also significantly improved. A very important advantage of this technique is that by the continuous potential cycling, the ring electrode surface is kept clean and unlike the “constant ring potential” experiments, no sensitivity loss can be experienced. (The curve of Figure 7(c) represents multiple overlaying ring CVs while in Figure 6(c) only a segment of the (continuously changing) ring currents was shown.)



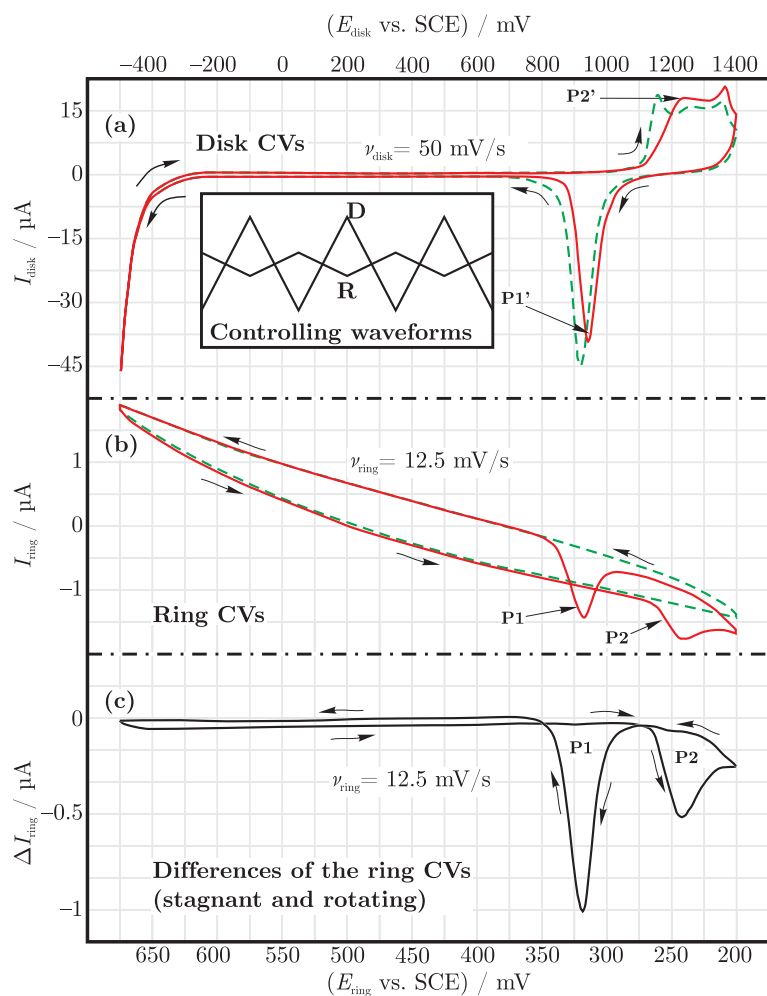


**Figure 7:** Multiple consecutive (however overlaying) cyclic voltammograms obtained simultaneously from the disk (a) and the ring (b) electrodes. Solid (red) and dashed (green) lines mark the measured CVs when the electrode is rotating (at  $500 \text{ min}^{-1}$ ) and when it is stagnant, respectively. The plot in (c) shows the difference between the solid and dashed curves in (b).

Based on the application of this method we can confirm the results found in the literature that the reducible (oxidized gold [5, 19]) species responsible for the peaks appearing in the ring current are mainly produced during the reduction of the 2D surface oxide layer (see peak P1' on the disk CV of Figure 7(a)); however we can also point out that the formation of the surface oxide yields reducible side-products as well (see peak P2' in Figure 7(a)).

### 3.2 Creating 3D maps of electrode reactions by dual dynamic measurements at an RRDE

**Experimental.** Experiments described in this section were carried out exactly as described in Section 3.1 with the difference that the  $0.5 \text{ mol dm}^{-3}$  sulphuric acid solution, in which the measurements were taking place, was saturated with air.

The capability of our measuring system to carry out dual potentiodynamic measurements has also been utilized for studying the oxygen reduction process (ORP, [20]) on a polycrystalline  $\text{Au}|\text{H}_2\text{SO}_4$  electrode. The ORP at gold surfaces has been extensively studied in the literature, and it has been established that in acidic media, the process usually involves the formation of hydrogen peroxide. The peroxide intermediate is reduced to water only at more negative potentials. Whether the  $2e^-$  or the  $4e^-$  process is more favourable on a polycrystalline gold surface is known to be a function of the electrode potential and the pH; however, to identify the potential region at which the two-electron pathway is dominant is not always straightforward. The application of the dual potentiodynamic perturbation technique makes it possible to estimate the disk potential at which the maximum amount of peroxide is formed, and thus can yield useful information regarding this matter. The general idea of the experiment is to apply a slow rate linear sweep perturbation to the disk electrode potential, while recording cyclic voltammograms of a high sweep-rate from the ring. The

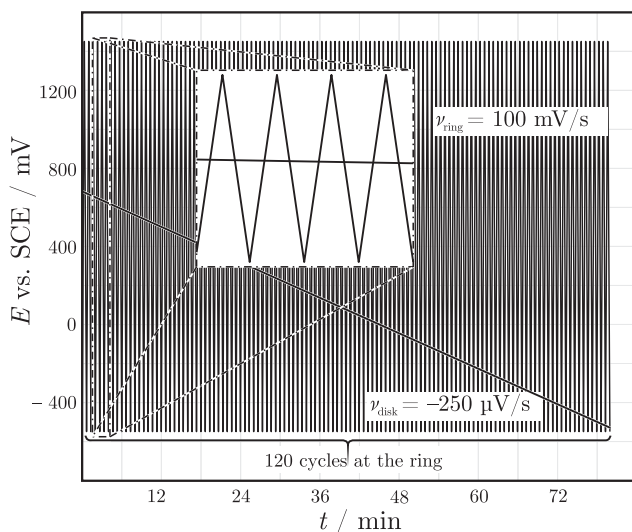


**Figure 8:** Controlling waveforms of the disk and ring electrodes: while the disk potential is slowly swept towards cathodic values, a multitude of cyclic voltammograms are obtained from the ring with a high sweep rate. Figure adapted from [6].

applied perturbing waveforms were those presented in Figure 8: the disk electrode was slowly polarized from 600 to  $-600$  mV vs. SCE (at a sweep rate of  $0.25$  mV/s), while the cyclic voltammograms of the ring were recorded at a sweep rate of  $100$  mV/s between the potential limits of  $1450$  and  $-550$  mV. The electrode was rotated at  $1000$   $\text{min}^{-1}$  during the experiment. Measured results (the polarization curve of the disk as well as the recorded ring CVs) are shown in Figure 9.

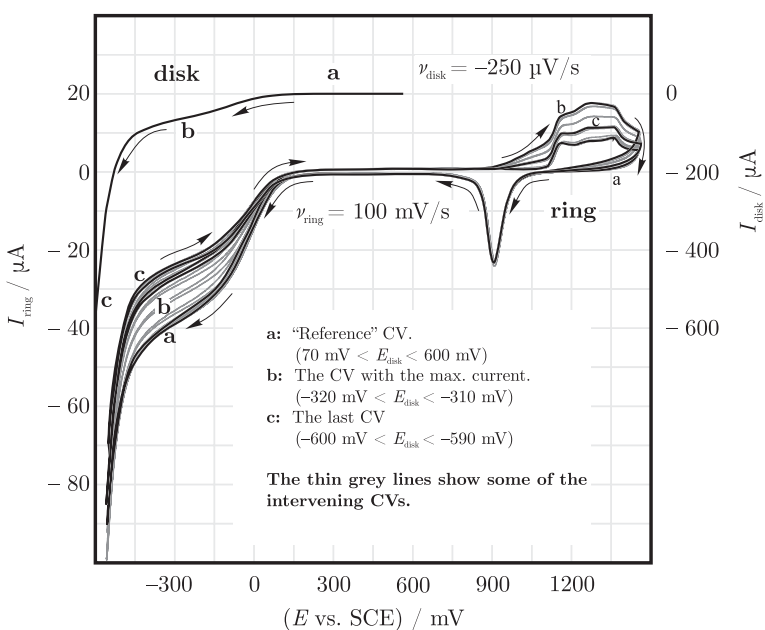


**Figure 9:** The shape of the CVs measured on the ring change when oxygen reduction occurs on the disk electrode in an air saturated  $0.5$   $\text{mol dm}^{-3}$  sulphuric acid solution. The polarization curve obtained from the disk and a few ring CVs are shown together. Figure adapted from [6].

At the beginning of the disk scan, while the disk potential is more positive than the negative potential limit of the double-layer region (section a), the cyclic voltammograms measured at the ring are characteristic for a clean polycrystalline Au electrode, and show no “collection-related” effects. However, as the disk potential becomes more and more negative (section b), significant changes of the ring CVs can be observed. One of these observable features is that the absolute values of the cathodic ring currents measured at negative ring potentials begin to decrease as the reduction of oxygen begins on the disk. This effect is termed shielding, and is a result of the fact that with decreasing disk potentials, the oxygen content of the solution reaching the ring electrode also decreases. The intensity of shielding thus indicates the lack of oxygen in the solution that is caused by the disk electrode process.

Apart from the shielding effect, signs of actual collection can also be seen on the ring CVs of Figure 9. This effect can be seen at positive ring potentials in the form of an anodic current. The anodic current is attributed to the fact that the hydrogen peroxide formed at the disk can get oxidized on the ring electrode if its potential is positive enough. The signal begins to appear as the disk potential gets to approximately  $70$  mV, and increases continuously until the disk potential reaches the value of approximately  $-310$  mV. However, a notable feature of this effect is that as the disk potential gets even more negative and enters section c, the measured ring signals begin to decrease again.

The results of Figure 9 can be better visualized if we plot the changes of the ring currents as a function of the

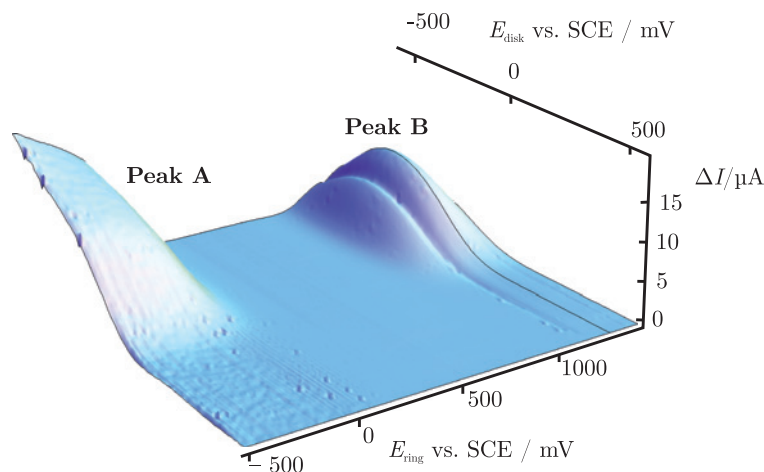


**Figure 10:** 3D map of the oxygen reduction process on poly-crystalline gold in  $0.5 \text{ mol dm}^{-3}$  sulphuric acid solution showing (peak A) the shielding of the ring that arises from the reduction of oxygen at the disk, and (peak B) an anodic peak that is caused by the oxidation of the hydrogen-peroxide formed at the disk. Figure adapted from [6].

disk and ring potentials in form of a three-dimensional surface such as that shown in Figure 10 [4, 6, 7].

### 3.3 RRDE Studies based on capacitance measurements on the ring electrode

So far we only presented RRDE studies that were based on the detection of faradaic currents at the ring electrode, although the RRDE configuration can be used in an essentially non-faradaic detection mode as well [8].

Let us consider the case when an electrochemical reaction taking place on the generator yields only products which are neither reducible nor oxidable on the collector in a reasonable potential range. These products, under steady-state conditions, should not be detectable as they cannot be involved in any charge transfer reaction. This does not mean, however, that the species may not interact with the collector electrode at all: the species can, for example, modify the structure of the electrical double-layer, which can occur by means of specific adsorption, by changing the concentrations in the diffuse double layer, etc. Such effects are, in principle, detectable by measuring the *ac* capacitance of the collector electrode. In what follows we present the use of this technique for studying the overoxidation of a conductive polymer, poly(3,4-ethylenedioxythiophene) (PEDOT) [21, 22].

The electrochemical and mechanical properties of thin PEDOT films deposited on gold have already been investigated in aqueous sulfuric acid solutions [23, 24]. It was shown that a sufficiently positive electrode potential ( $E > 800 \text{ mV vs. SCE}$ ) may lead to the overoxidation of the polymer. The structural changes that accompany this process result in a distorted electrochemical and mechanical behaviour, as observed by surface

stress measurements, cyclic voltammetry, electrochemical impedance spectroscopy, and by scanning electron microscopy (SEM) [23, 24]. Apart from the morphological changes, overoxidation can also affect the charge structure of the polymer film. PEDOT is a redox conductive polymer that incorporates counter-ions from the surrounding electrolyte solution in order to maintain electroneutrality, thus its charging processes may involve a detectable counter-ion flux leaving the film [25, 26].

For this reason, the Au|PEDOT| $0.1 \text{ mol dm}^{-3} \text{ H}_2\text{SO}_4$  electrode seems to be a promising target for studying the counter-ion flux accompanying the charging and discharging processes, as well as the degradation of the polymer film. Similar studies have already been carried out by the use of rotating ring–disk electrodes [27–29], but these were confined to target systems where electrochemically oxidable (usually halide) counter-ions were involved in the flux, providing means for faradaic detection. Sulphate, the most predominant counter-ion in the system studied here, is not detectable by such means; yet it may be specifically adsorbed on a bare gold ring [30] at well-chosen potentials, causing measurable changes of the interfacial capacitance.

**Experimental.** Measurements presented in this section were carried out with the same gold disk/gold ring RRDE (PINE AFE7R8AuAu) as in the previous sections. Prior to the measurements, the disk was covered with PEDOT under galvanostatic conditions. All the glass parts of the cell were thoroughly cleaned by Caro's acid, a subsequent rinsing with MilliQ water and by vapour steam cleaning. Prior to the polymer deposition, the RRDE tip was mirror-polished first by the use of SiC paper, then with a diamond suspension (finest grain size:  $0.1 \mu\text{m}$ ). After polishing, the electrode surfaces were rinsed with MilliQ water and cleaned by ultrason-

ication. The deposition of PEDOT took place in a standard three-electrode cell at room temperature under an inert gas (Ar) blanket. The depositing solution contained  $0.01 \text{ mol dm}^{-3}$  of the monomer (EDOT, analytical grade, Aldrich) and  $0.1 \text{ mol dm}^{-3}$  of sodium sulphate (analytical grade, Fluka). Only the RRDE disk served as a substrate for the deposition, the ring electrode was covered by a tight Teflon cap, preventing it from any contact with the monomer solution. A Pt wire was used as an auxiliary electrode, and a KCl saturated calomel electrode (SCE) was used as a reference. The galvanostatic deposition lasted 30 min at a current density of  $200 \mu\text{A cm}^{-2}$ . A commercial potentiostat (AutoLab PGSTAT 20) was used for this purpose. Before the actual measurements had taken place, the electrode tip was held in MilliQ water for a few days in order to remove any residuals of the monomer. The RRDE measurements were then carried out in a  $0.1 \text{ mol dm}^{-3}$  sulphuric acid solution (analytical grade, Merck). The solution was purged by Ar and the measurements took place in an Ar atmosphere. A gold sheet with large surface area was used as an auxiliary electrode, and NaCl-saturated calomel (SSCE) was applied as a reference. The reference electrode compartment was separated from the rest of the cell by a Luggin probe.

The operating principle of the applied measurement method is that while the disk electrode potential is

arbitrarily controlled, a small-signal sinusoid voltage perturbation of a given frequency  $f$  is applied to the ring. Determining the capacitance of the ring electrode ( $C_{\text{ring}}$ ) is in this case possible by a synchronized sampling of the ring current and potential. Both of these are sinusoid signals, and by determining the ratio of their amplitudes and the phase shift between them, the impedance (and, subsequently, the capacitance) of the electrode can be calculated [8].

In case of the measurements presented in Figure 11 the ring potential was set to a 600 mV vs. SSCE  $dc$  level and a sine-wave perturbation (frequency: 20 Hz, amplitude: 5 mV) was applied to it. In the meantime, several cyclic voltammograms were recorded on the disk electrode. The lower vertex of these CVs was set to  $-200 \text{ mV}$  vs. SSCE and the applied sweep-rate was  $10 \text{ mV/s}$ . After recording a few potential cycles with the same parameters, the upper vertex potential of the cycles was gradually increased (from 600 to 800, then to 1200 mV, as shown by the green curve in Figure 11). Increasing the upper vertex potential to above 800 mV has triggered strong anodic currents on the disk, indicating the overoxidation and subsequent degradation of PEDOT. This is visualized by the CVs, as well as by the SEM images in the insets of Figure 11.

The calculated ring capacitance shows a net decrease with time: this is probably due to a continuous adsorption of some organic species to the electrode surface. However,

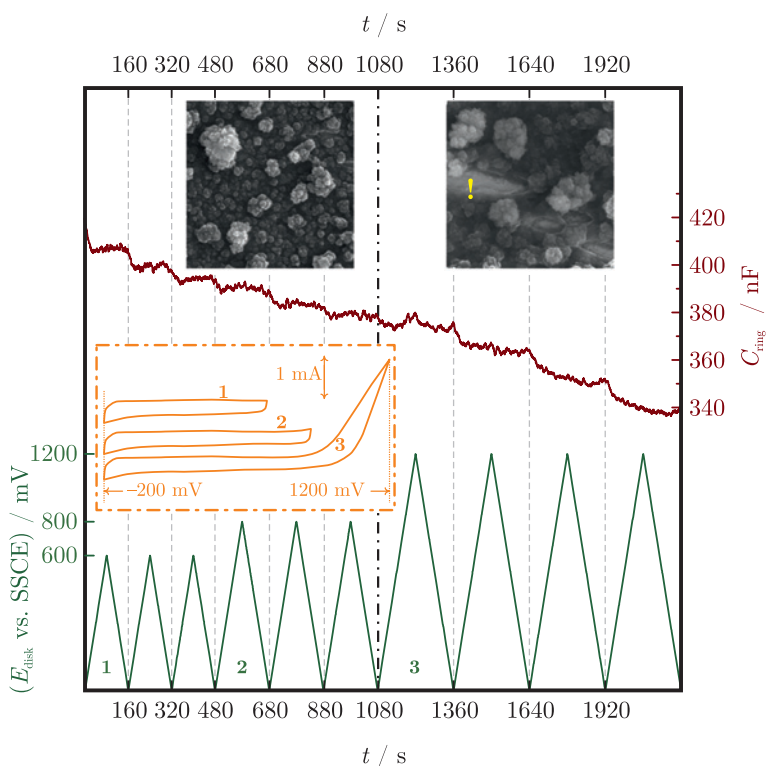


**Figure 11:** Changes of the ring capacitance (red curve, calculated by the sine-wave correlation method described in [8]), as the disk is polarized with triangular sweeps of different upper vertices (green triangles). Selected cyclic voltammograms are shown in the orange box inset. The RRDE was rotated at  $500 \text{ min}^{-1}$  during the experiment. SEM images (measured ex-situ on a different gold substrate) demonstrate the effect of film degradation: after polarizing the disk electrode to 1200 mV, the film degrades, and the underlying gold surface becomes partially visible (see the exclamation mark in the SEM image to the right). Figure adapted from [8].

a closer inspection of this curve reveals a certain periodicity with the applied disk potential; the ring capacitance curve shows local maxima when the disk electrode is negatively polarized. This effect becomes more obvious after a slight overoxidation of the PEDOT film, which can be interpreted as a result of the increasing film surface area and/or the effect of free gold surfaces becoming available due to the degrading polymer film. (See also the SEM images in the insets of Figure 11.)

Interpreting this behaviour is possible by assuming that at sufficiently positive potentials the increased porosity of the film and the free gold surfaces may provide new adsorption sites for the sulphate counter-ions in the electrolyte solution, while at more negative potentials they may release the previously adsorbed sulphate. This effect can account for the temporary increases of the measured ring capacitance (indicating sulphate flux), as shown in Figure 11. For more details of this measurement, see [8].

## 4 Summary

In this paper we gave an overview of a measurement apparatus capable to carry out bi-potentiodynamic measurements on rotating ring–disk electrodes and by reviewing the previous work of our research group [4–8] we attempted to demonstrate the advantages of this novel measurement technique.

By using a rotating gold ring–gold disk| $0.5 \text{ mol dm}^{-3}$   $\text{H}_2\text{SO}_4$  electrode setup, we were able to show that during the reduction of the surface oxide layer of gold at least one soluble, electroreducible gold species is escaping from the disk electrode, and we demonstrated that the potentiodynamic control of both electrodes is essential for carrying out reproducible measurements [5, 7].

The method of dual potentiodynamic scanning was also used to study the oxygen reduction reaction as it occurs on a gold ring–gold disk| $0.5 \text{ mol dm}^{-3}$   $\text{H}_2\text{SO}_4$  electrode. This method was capable of a direct monitoring of the formation of  $\text{H}_2\text{O}_2$  as a function of the disk potential during oxygen reduction and we showed that the new 3D representation of the data can be effectively used in order to reveal the formation of electroactive species in a disk electrode reaction [6, 7].

By the application of *ac*-perturbation based detection to a PEDOT-modified disk electrode in combination with a bare gold ring, it was also shown that the measured ring capacitance changes can be correlated to the polarization of the polymer film, thus an RRDE can also be effectively used for the monitoring of processes that do not yield any oxidable/reducible intermediates [8].

In general, the simultaneous perturbation of the disk and ring electrode potentials of an RRDE with time-varying controlling waveforms seems to be an effective way of carrying out high-sensitivity collection experiments that can yield useful information on the mechanisms of various electrochemical processes.

**Acknowledgement:** This research has received funding from the Hungarian Scientific Research Fund (OTKA) under Grant Agreement № K109036.

The work was supported by the ÚNKP-16-3 New National Excellence Program of the Ministry of Human Capacities, Hungary (ELTE/8495/60(2016)).

S. Vesztergom gratefully acknowledges the support of the European Union and the State of Hungary, as well as the co-financing of the European Social Fund in the framework of TÁMOP 4.2.4. A/1-11-1-2012-0001 “National Excellence Program”.

## References

1. Brett CMA, Brett AMO (1993) *Electrochemistry — Principles, Methods and Applications*. Oxford University Press, Oxford
2. Bard AJ, Faulkner LR (2001) *Electrochemical Methods. Fundamentals and Applications*. John Wiley & Sons, New York
3. Oldham KB (2011) Trends in electrochemical instrumentation and modeling. *J Solid State Electrochem* 15:1967–1698
4. Vesztergom S, Láng GG (2013) The construction of a novel electrochemical measuring system for enhanced rotating ring–disk electrode experiments. *Instrum Sci Technol* 41:82–95
5. Vesztergom S, Ujvári M, Láng GG (2011) RRDE experiments with potential scans at the ring and disk electrodes. *Electrochem Commun* 13:378–381
6. Vesztergom S, Ujvári M, Láng GG (2012) RRDE experiments with independent potential scans at the ring and disk electrodes — 3D map of intermediates and products of electrode processes. *Electrochem Commun* 19:1–4
7. Vesztergom S, Ujvári M, Láng GG (2013) Dual cyclic voltammetry with rotating ring–disk electrodes. *Electrochim Acta* 110:49–55
8. Kovács N, Ujvári M, Broekmann P, Vesztergom S (2015) Characterization of the capacitance of a rotating ring–disk electrode. *Instrum Sci Technol* 43:633–648
9. Albery WJ, Hitchman ML (1971) *Ring–Disc Electrodes*. Oxford University Press, London
10. Müller L (1972) Die rotierende Scheibenelektrode mit Ring und ihre Anwendungsmöglichkeiten. *Z Chem* 12:209–219
11. Frumkin AN, Nekrasov LN, Levich VG, Ivanov YB (1959) Die Anwendung der rotierenden Scheibenelektrode mit einem Ring zur Untersuchung von Zwischenprodukten elektrochemischer Reaktionen. *J Electroanal Chem* 1:84–89
12. Napp DT, Johnson DC, Bruckenstein S (1967) Simultaneous and independent potentiostatic control of two indicator electrodes. *Anal Chem* 39:481–485

13. Pine Instruments Company (1992) Operating Instructions for AFRDE5 Potentiostat. Grove City PA
14. ZAHNER-Elektrik GmbH & CoKG (2010) External Potentiostats Installation and Operation Manual. Kronach
15. National Instruments (2008aa) NI 446x Specifications. Austin TX
16. National Instruments (2008b) NI 6013/6014 User Manual. Austin TX
17. Johnson GW (2007) LabVIEW Graphical Programming: Practical Applications in Instrumentation and Control. McGraw–Hill, New York
18. Cadle SH, Bruckenstein S (1974) Ring–disk electrode study of the anodic behavior of gold in 0.2 M sulfuric acid. *Anal Chem* 46:16–20
19. Cherevko S, Topalov AA, Katsounaros I, Mayrhofer KJJ (2013) Electrochemical dissolution of gold in acidic medium. *Electrochim Commun* 28:44–46
20. Yeager E (1986) Dioxygen electrocatalysis: Mechanism in relation to catalyst structure. *J Mol Catal* 38:5–25
21. Inzelt G (2012) *Conducting Polymers: A New Era in Electrochemistry*. Springer, Heidelberg
22. Láng GG, Ujvári M, Vesztergom S, Kondratiev V, Gubicza J, Szekeres KJ (2016) The electrochemical degradation of poly(3,4-ethylenedioxythiophene) films electrodeposited from aqueous solutions. *Z Phys Chem* 230:1281–1302
23. Láng GG, Ujvári M, Bazsó F, Vesztergom S, Újhelyi F (2012) In-situ monitoring of the electrochemical degradation of polymer films on metals using the bending beam method and impedance spectroscopy. *Electrochim Acta* 73:59–69
24. Ujvári M, Gubicza J, Kondratiev V, Szekeres KJ, Láng GG (2015) Morphological changes in electrochemically deposited poly(3,4-ethylenedioxythiophene) films during overoxidation. *J Solid State Electrochem* 19:1247–1252
25. Andrieux CP, Savéant JM (1988) Electroneutrality coupling of electron hopping between localized sites with electroinactive counterion displacement. Part 1. — Potential-step plateau currents. *J Phys Chem C* 92:6761–6767
26. Lovrić M, Scholz F (1999) A model for the coupled transport of ions and electrons in redox conductive microcrystals. *J Solid State Electrochem* 3:172–175
27. Pickup PG, Osteryoung RA (1985) Charging and discharging rate studies of polypyrrole films in  $\text{AlCl}_3 : 1\text{-methyl-(3-ethyl)-imidazolium chloride}$  molten salts and in  $\text{CH}_3\text{CN}$ . *J Electroanal Chem* 195:271–288
28. Shinohara H, Kojima J (1989) Electrically controlled ion transfer and pH change near a conducting polymer-coated electrode. *J Electroanal Chem* 266:297–308.
29. Salzer CA, Elliott CM (1999) Quantitative in situ measurement of ion transport in polypyrrole/poly(styrenesulfonate) films using rotating ring–disk voltammetry. *Anal Chem* 71:3677–3683
30. Pajkossy T, Wandlowski T, Kolb DM (1996) Impedance aspects of anion adsorption on gold single crystal electrodes. *J Electroanal Chem* 414:209–220

## Bionotes

### Soma Vesztergom

Eötvös Loránd University, Department of Physical Chemistry, Pázmány Péter sétány 1/A, 1117 Budapest, Hungary  
 vesztergom@chem.elte.hu

### Noémi Kovács

Eötvös Loránd University, Department of Physical Chemistry, Pázmány Péter sétány 1/A, 1117 Budapest, Hungary

### Mária Ujvári

Eötvös Loránd University, Department of Physical Chemistry, Pázmány Péter sétány 1/A, 1117 Budapest, Hungary

### Győző G. Láng

Eötvös Loránd University, Department of Physical Chemistry, Pázmány Péter sétány 1/A, 1117 Budapest, Hungary